Chapter 5
Control of Power of a DFIG Generator with MPPT Technique for Wind Turbines Variable Speed

Yasmine Ihedrane, Chakib El Bekkali, Badre Bossoufi, and Manale Bouderbala

Abstract This chapter presents the study and the modeling of a variable speed wind system based on Doubly Fed Induction Generator controlled by a linear control type PI, in order to independently control the active and reactive stator powers generated by the wind turbine system.

The proposed control is applied to a Doubly Fed Induction Generator whose stator is directly connected to the grid in contrast to the rotor which is connected via "Back-to-Back" converters.

The objective of the modeling is to apply the direct and indirect control of the active and reactive power generated by the wind turbine based on the Doubly Fed Induction Generator via the Maximum Power Point Tracking (MPPT) strategy, to extract the maximum power from the wind.

Simulation results are tested and compared in order to evaluate the performance of the proposed system.

Keywords Doubly fed induction generator (DFIG) · Wind turbine · Direct field oriented control (DFOC) · Indirect field oriented control (IFOC) · Maximum power point tracking (MPPT)

5.1 Introduction

Today, energy demands has increased enormously. Fossil fuel sources are declining and the preoccupations concern the levels of pollution in the environment are the main drivers for electricity generation from renewable energy sources.

Y. Ihedrane (✉) · C. E. Bekkali
Laboratory of STIC, Faculty of Sciences Dhar El Mahraz, Sidi Mohamed Ben Abdellah University, Fez, Morocco

B. Bossoufi · M. Bouderbala
Laboratory of Electrical Engineering and Maintenance, Higher School of Technology, EST-Oujda, University of Mohammed I, Oujda, Morocco

N. Derbel, Q. Zhu (eds.), *Modeling, Identification and Control Methods in Renewable Energy Systems*, Green Energy and Technology,
https://doi.org/10.1007/978-981-13-1945-7_5

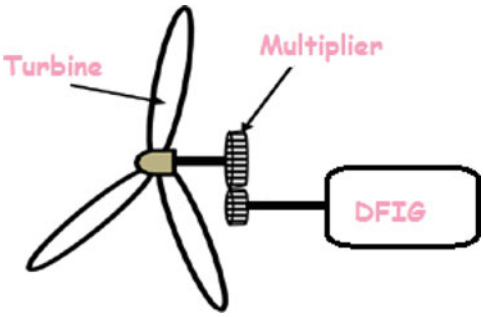

Fig. 5.1 Wind conversion chain

Renewable energies, such as solar energy and wind energy, are clean, inexhaustible energies, because of all these factors there has been a great deal of interest in wind power generation in recent years (Kazemi and Kojabadi 2010).

The induction machine in variable speed drives poses some difficulties which make its control more complex compared to a DC machine. Indeed, this type of machine is characterized by a multivariable, nonlinear mathematical model, with a strong coupling between the two control variables, which are the magnetic Field and the electromagnetic torque (de Wit 2000). In other words, it is not possible to control independently the input variables (voltage or current). Moreover, some state variables are not accessible to measurements, and its parameters are subject to variations over time. For this reason, several methods of controlling the DFIG have emerged, among them, the field oriented control technique.

The principle of this technique was developed by BLASCHKE in the early 1970s; it consists in orienting the field along one of the axes of the referential d, q in order to make this machine's behavior similar to that of a Separately Excited DC Machine. This control is based on PI controllers.

In this chapter, we begin with the modeling of the turbine. Next, a tracking technique operating point at maximum power point tracking (MPPT) will be presented (Bekakra and Attous 2011; Ghoudelbourk et al. 2016). Then, we will present a model of the DFIG in the referential (d, q). After that, we will tackle the principle of field oriented control. Finally with the use of MATLAB/SIMULINK, we will present and analyze the simulation results to validate our theoretical study.

5.2 Modeling of the Wind Conversion Chain

The turbine studied in this chapter comprises three blades of length R. They are fixed on a drive shaft rotating at a turbine speed Ω_t connected to a gain multiplier G which drives an electric generator as shown in Fig. 5.1 (Ihedrane et al. 2017a).

5.2.1 Model of the Turbine

5.2.1.1 Turbine Power

The kinetic power of the wind is defined by the following equation (Ihedrane et al. 2017a,b)

$$P_v = \frac{\rho \times S \times V^3}{2} \tag{5.1}$$

where:

ρ: Density of the air

S: Surface swept by the turbine

v: Wind Speed

The turbine can convert only a percentage of the wind power presented by the coefficient C_p, hence the expression of the aerodynamic power can be described as follows:

$$P_{aero} = C_p(\lambda, \beta) \times \frac{\rho \times S \times V^3}{2} \tag{5.2}$$

5.2.1.2 Power Coefficient

The power coefficient $C_p(\lambda, \beta)$ represents the aerodynamic efficiency of the wind turbine. The latter depends on the specific speed λ and the angle of the orientation of the blades β. It is approximated by the following function (Bossoufi et al. 2014; Ihedrane et al. 2017a):

$$C_p(\lambda, \beta) = C_1 \times \left(\frac{C_2}{A} - C_3 \times \beta - C_4\right) \times \exp\left(-\frac{C_5}{A}\right) + C_6 \times \lambda \tag{5.3}$$

where: $\frac{1}{A} = \frac{1}{(\lambda + 0.08 \times \beta)} - \frac{0.035}{\beta^3 + 1}$

5.2.1.3 Specific Speed

Specific speed λ is defined as the ratio of the linear turbine speed and the wind speed (Ihedrane et al. 2017a; Youcef 2014), it is given by (5.4):

$$\lambda = R \times \frac{\Omega_t}{V} \tag{5.4}$$

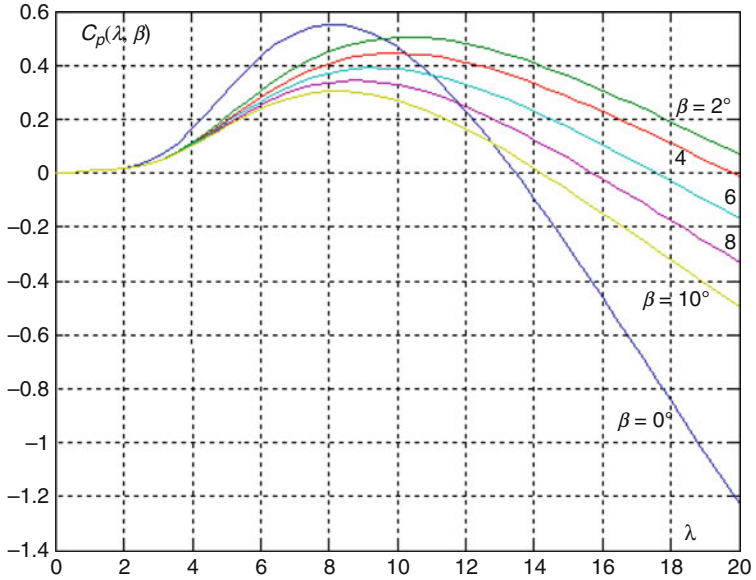

Fig. 5.2 Power coefficient C_P in function of speed ratio λfor different values of β

Figure 5.2 shows the variation of power coefficient C_P in function of speed ratio λ for different values of β (Bossoufi et al. 2014; Ihedrane et al. 2017a). From this figure we can note that the power coefficient C_p reaches its maximum 0.5506 for a speed ratio $\lambda_{opt} = 8$ and $\beta = 0°$.

5.2.1.4 Mechanical Torque

From the expression of the power produced by the turbine and knowing the speed turbine, the mechanical torque can be expressed by 5.5 (Ihedrane et al. 2017a):

$$C_{aero} = \frac{P_{aero}}{\Omega_t} = C_p(\lambda, \beta) \times \frac{\rho \times S \times V^3}{2 \times \Omega_t} \tag{5.5}$$

5.2.2 Model of the Multiplier

The multiplier transforms the turbine speed into the generator speed and the aerodynamic torque into the generator torque according to the following system (Ihedrane et al. 2017a; Youcef 2014):

$$\begin{cases} \Omega_t = \dfrac{\Omega_{mec}}{G} \\ C_g = \dfrac{C_{aero}}{G} \end{cases} \tag{5.6}$$

where:

Ω_{mec}: rotation speed of the generator.

C_g: The generator torque.

5.2.3 Dynamic Equation of the Transmission Shaft

From the mechanical torque exerted on the rotor shaft of the wind turbine and the electromagnetic torque C_{em}, the fundamental equation of the dynamics makes it possible to determine the evolution of the mechanical speed (Guda 2005):

$$C_{mec} = J\frac{d\Omega_t}{dt} = C_g - C_{em} - C_f \tag{5.7}$$

with:

J: the total inertia, it is constituted by the turbine inertia J_t, and the generator inertia J_g (Aimani 2004):

$$J = \frac{J_t}{G} + J_g \tag{5.8}$$

The block diagram corresponding to the model of the turbine is given in Fig. 5.3.

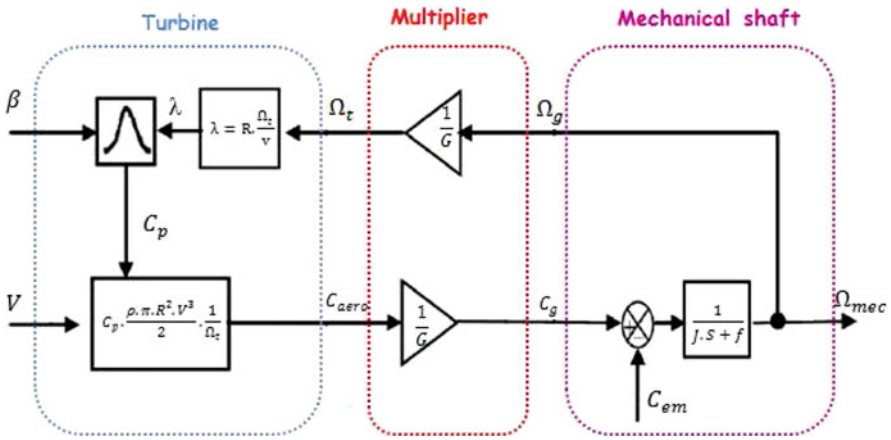

Fig. 5.3 Block diagram of the wind converter model

5.2.4 Control Strategy for Wind Turbine

5.2.4.1 Maximum Power Point Search Method

The characteristic of the optimal power of a wind turbine is strongly non-linear and "bell-shaped" (Johansen et al. 2001).

The wind system must find the maximum power, for each wind speed, which is equivalent to finding the optimum rotational speed.

Figure 5.4 illustrates the characteristic curves of the wind turbine in the plane (power,rotational turbine speed). Each curve corresponds to a wind speed V_v. The vertices of these characteristics present the optimal points sought which define a curve called the optimal power curve given by:

$$P_{opt} = C_p opt(\lambda_{opt}) \times \frac{\rho \times \pi \times R^2 \times V^3}{2} \tag{5.9}$$

The wind system requires a perfect tracking of the optimum power curve in order to have an ideal operation, to do that, a specific command called Maximum Power Point Tracking (MPPT) must be used. The strategy of this control consists in controlling the electromagnetic torque in order to adjust the mechanical speed in a way to maximize the electrical power generated.

There are two approaches:

- The first approach considers that the characteristic $C_p = f(\lambda)$ is not known (Johansen et al. 2001).
- The second one considers that the characteristic $C_p = f(\lambda)$ is known. Simply follow the optimum power curve for the wind turbine to be in optimum conditions.

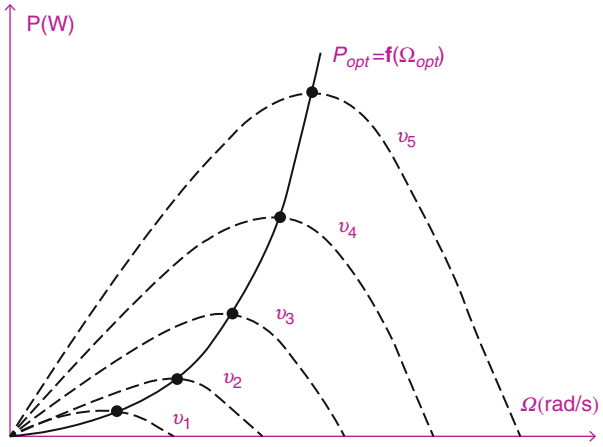

Fig. 5.4 Characteristics of the wind turbine in the plane (power,rotational turbine speed)

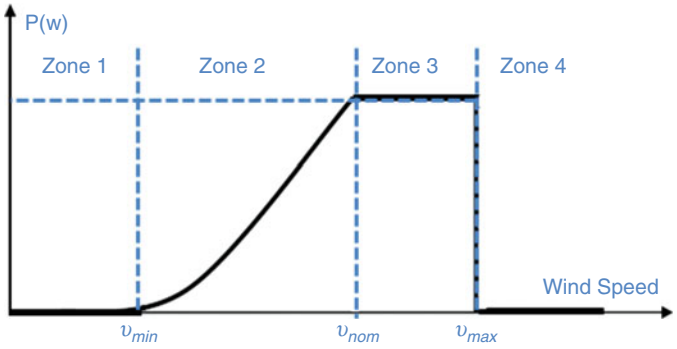

Fig. 5.5 Characteristics (Power, wind speed)

This approach Simplifies the algorithm of the maximum power and allows to use more basic and less expensive converters.

5.2.4.2 Operation of a Variable Speed Wind Turbine

Figure 5.5 illustrates the different operating phases of a variable speed wind turbine (Mourad 2016).

- Wind speeds are very low and insufficient to drive the wind turbine and produce power.
- the wedge angle is kept constant, and the control of the electromagnetic torque will be implemented in order to capture the maximum power for each wind speed (MPPT principle). In this zone, the generator power curve keeps a rapid progression (Mourad 2016).
- Zone 3: The generator speed is kept constant at its maximum as opposed to a suitable torque. The increase in the wind speed leads to a decrease in the coefficient C_p and a slower increase in the recovered power. When the maximum of the power generator is reached, the angle of the blades (pitch) is modified (Passage from β_1 to β_2) in order to degrade the coefficient C_p.
- Zone 4: In this zone, when the wind speed becomes too high V_M, an emergency device is used to stop the wind turbine (No electricity production) and to prevent damage.

5.2.4.3 Maximum Power Extraction Technique

In order to extract the maximum power from the wind turbine, we need an algorithm acting on the set point variables, to have a good efficiency of the device.

In the literature we have found two types of control structures for the maximization of power extracted:

- The MPPT control without mechanical speed control.
- The MPPT control with mechanical speed control

In this chapter we are interested in the MPPT control without mechanical speed control.

In practice, an exact measurement of wind speed is difficult to achieve. Due to the following reasons (Aimani 2004; Mourad 2016).

- The anemometer is located behind the rotor of the turbine, which gives an erroneous reading of the wind speed.
- Since the diameter of the surface swept by the blades is large (typically 70 m for a 1.5 m wind turbine), a significant variation in wind appears depending on the height of the anemometer. So, the use of a single anemometer leads to use only one local measurement of the wind speed which is therefore not sufficiently representative of its average value appearing on all the blades.

An incorrect measurement of the speed therefore necessarily leads to a degradation of the power captured according to the power extraction technique. This is why most wind turbines are controlled without speed control. This control structure is based on the assumption that the wind speed varies very steadily (Gaillard 2010):

$$J\frac{d\Omega_{mec}}{dt} = C_g - Cem - f \times \Omega_{mec} = 0 \tag{5.10}$$

According to this equation, and by neglecting the mechanical torque Cmec and the effect of the couple of viscous friction $f \times \Omega_{mec}$, we obtain the following equation:

$$C_{em} = C_g \tag{5.11}$$

The reference electromagnetic torque is determined from an estimation of the aerodynamic torque:

$$C_{emref} = \frac{C_{aeroref}}{G} \tag{5.12}$$

We know that:

$$\begin{cases} C_{aero} = C_p(\lambda, \beta)\dfrac{\rho \times \pi \times R^2 \times V^3}{2 \times \Omega_t} \\ \Omega_t = \dfrac{\Omega_{mec}}{G} \\ V_{est} = R\dfrac{\Omega_{test}}{2 \times \lambda_{test}} \end{cases} \tag{5.13}$$

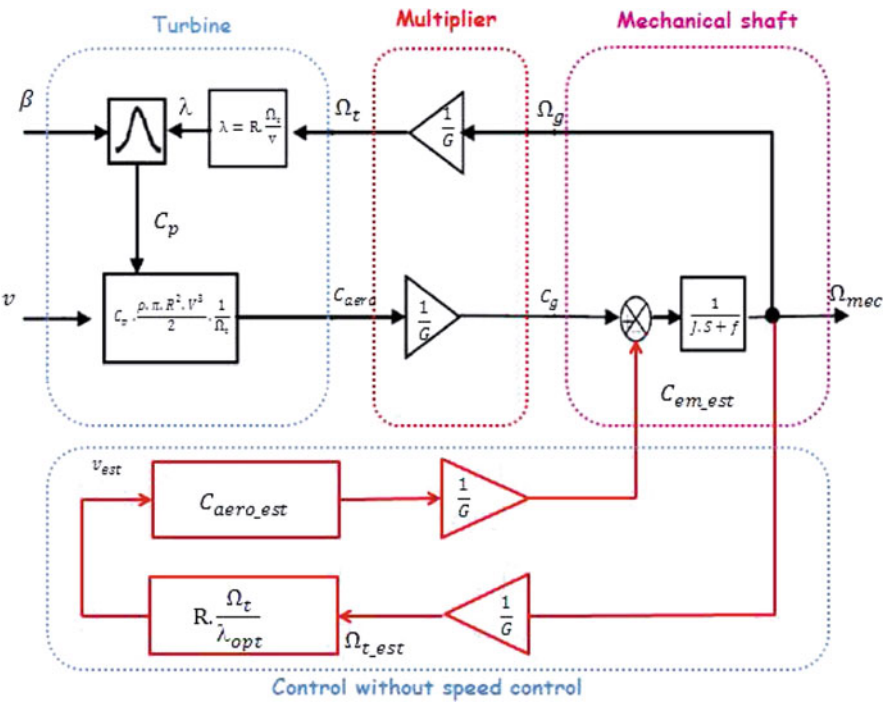

Fig. 5.6 Block diagram of the MPPT strategy without speed control

After calculation and a series of combinations, we get the following equation:

$$C_{emref} = \frac{C_p(\lambda, \beta)}{\lambda_{opt}^3} \times \frac{\rho \times \pi \times R^3}{2} \times \frac{\Omega_{mec}^3}{G^3} \tag{5.14}$$

The block diagram of the MPPT strategy without mechanical speed measurement is shown in Fig. 5.6.

5.3 Modeling of the Doubly Fed Induction Generator DFIG

5.3.1 Structure of the Electrical Machine

The wind turbine conversion system studied in this chapter is shown in Fig. 5.7. It is divided into two main parts which will be modeled separately: the Doubly Fed Induction Generator whose stator is directly connected to the grid, in contrast to the rotor which is connected to the grid via powers converters "Back to Back",

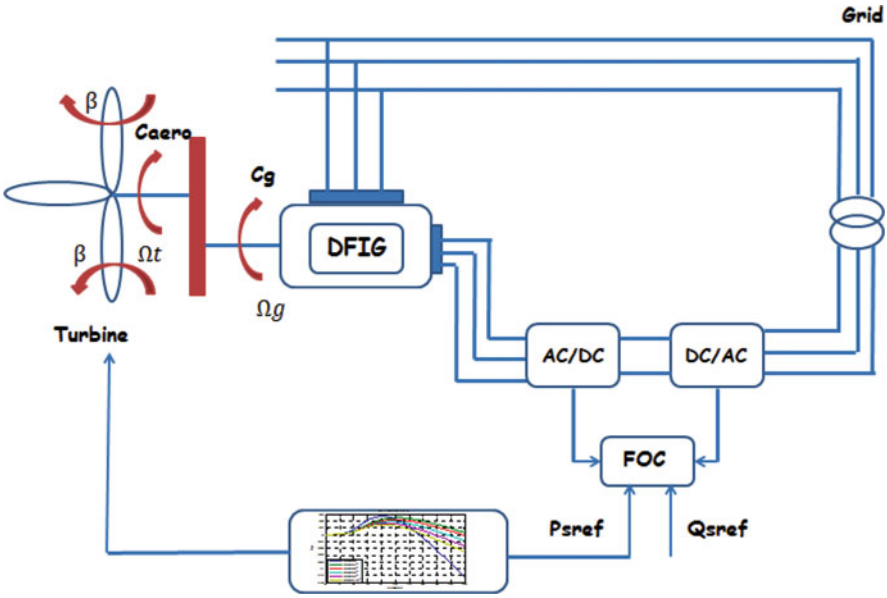

Fig. 5.7 General structure of a wind turbine conversion chain

these converters being able to operate as a rectifier or an inverter according to the direction of the energy transit.

This structure has been retained in this work, in order to establish a control strategies with the objective of controlling the power exchange between the generator and the electrical grid.

The stator magnitudes have the same frequency as that of the grid, that is why it is useless to use power converters to transfer the stator power. On the other hand, the rotor magnitudes don't have the same frequency as the alternating magnitudes of the grid, which depend on the speed of the rotor and consequently the wind speed, which justifies the use of a voltage converter feeding the rotor.

In the context of the production of electrical energy from wind power, this device can operate at fixed or variable speed, operate in hypo-synchronous or hyper-synchronous mode.

The powers converter side generator allows the control of the active and reactive power produced by the DFIG, and the powers converter side grid allows the control of the DC bus voltage and the power factor at the connection of the wind turbine with the power grid (Datta 2002).

The use of a doubly Fed Induction Generator presents an excellent compromise between the range of speed variation and the dimensioning of the converters compared to the nominal power of the machine.

5.3.2 *Operation of the Doubly Fed Induction Machine in Generator Mode*

The Doubly Fed Induction Machine, unlike other electrical machines, is reversible and can operate in generator mode and motor mode.

Figure 5.8 shows the form of the mechanical torque/speed characteristic of the induction machine (Mourad 2016).

From Fig. 5.8 it can be seen that the induction machine operates in motor mode for $g > 0$ and in generator mode in the opposite case.

For operation with Doubly fed Induction Machine, the stator is powered by a first balanced three-phase voltage source of frequency f, the rotor is connected to a second alternating frequency source f_r.

The currents flowing in the stator windings create rotating field at the speed $\Omega_s = \frac{\Omega_s}{P}$, similarly, the rotor currents produce a rotor field rotating at a speed $\Omega_r = \frac{\Omega_r}{P}$.

When the rotating field of the ror rotates in the same direction of rotation of the stator field, the slip 'g' is positive and the rotor rotates slower than the stator field $\Omega < \Omega_s$, so, the machine operates in Hypo-Synchronous mode.

In the opposite case, the rotating field created by the windings of the rotor rotates in the opposite direction than that of the stator, the slip 'g' becomes negative and the rotor rotates faster than the rotating field created by the stator $\Omega > \Omega_s$, so, the machine operates in hyper-synchronous mode.

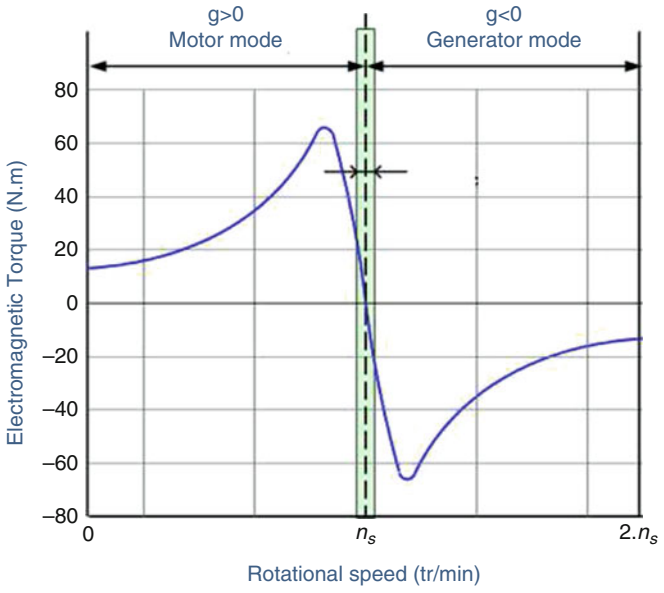

Fig. 5.8 Torque/speed characteristic of the induction machine

For the conventional induction machine, a positive sign of slip 'g' corresponds to a motor operation of the machine, whereas a negative sign translates to a generator operation, which may lead to confusion in the understanding of the DFIM operating principle, in which the sign of the slip reflects hypo or hyper-synchronous operation and not the operating mode of the machine (motor or generator) (Bennani 2011).

The possibility of operating in hyper-synchronism or in hypo-synchronism, both in motor mode and in generator mode, is obtained by controlling the amplitude and phase of the rotor voltages, these making it possible to control the magnetic field at inside the machine.

5.3.3 Modeling of the Doubly Fed Induction Generator

5.3.3.1 Simplifying Assumptions

The basic structure of the three-phase induction machine is given by Fig. 5.9.

Despite its simplicity of construction, the mathematical model of the Doubly Fed Induction Gnerator DFIG is complex. In the three-phase referential fixed and linked to the stator, the model of the induction machine present the disadvantage of arriving at differential equations with variable coefficients as a function of the position of the rotor, and therefore of time.

To remediate to this problem, several approaches have been used, among them the approach based on the theory of the two axes RH Park (Park 2012) which

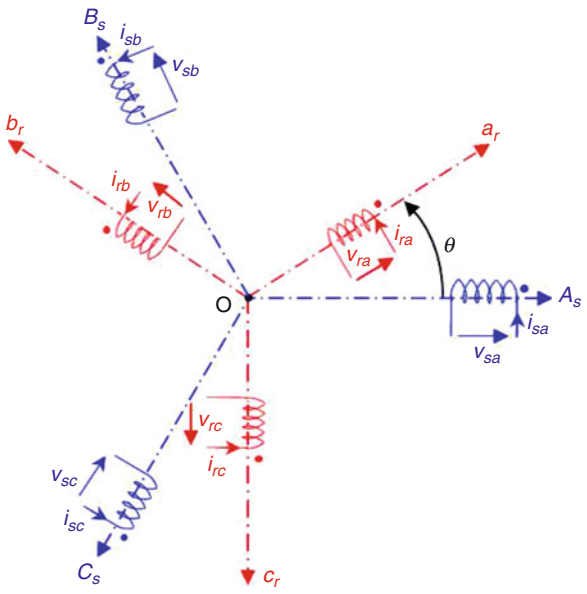

Fig. 5.9 Structure of the three-phase induction machine

consists in transforming the three-phase system into an equivalent two-phase system, moving from the fixed frame of reference (A, B, C) to a second mobile reference frame (d, q): 'd' presents the direct axis and 'q' the quadrature axis, perpendicular and mutually coupled, the angle between the two referential is called 'the Park angle'.

5.3.3.2 Application of Park Transformation to DFIG

Figure 5.10 presents the DFIM model in the PARK referential.

From Fig. 5.10 we obtain:

$$\theta_s = \theta_r + \theta \tag{5.15}$$

So its derivative can be writing as follows:

$$\frac{d\theta_s}{dt} = \frac{d\theta_r}{dt} + \frac{d\theta}{dt} \tag{5.16}$$

The modeling of the DFIG is identical to that of the induction machine cage. The only difference lies in the fact that the rotor voltages are not null because these windings are not 'short-circuited'.

The general equations obtained after the application of the Park transformation are given by the following equations.

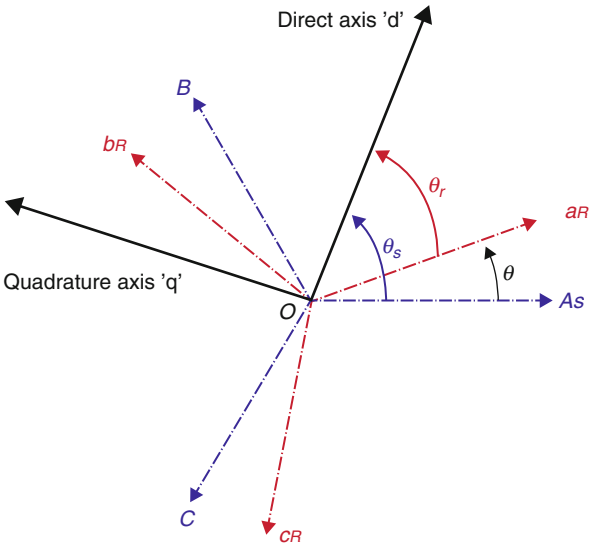

Fig. 5.10 Graphical representation of DFIG in the park referential

- Stator Voltages:

$$\begin{cases} V_{sd} = R_s \times I_{sd} + \dfrac{d\Phi_{sd}}{dt} - \omega_s \times \Phi_{sq} \\ V_{sq} = R_s \times I_{sq} + \dfrac{d\Phi_{sq}}{dt} + \omega_s \times \Phi_{sd} \end{cases} \tag{5.17}$$

- Rotor Voltages:

$$\begin{cases} V_{rd} = R_r \times I_{rd} + \dfrac{d\Phi_{rd}}{dt} - \omega_r \, \Phi_{rq} \\ V_{rq} = R_r \times I_{rq} + \dfrac{d\Phi_{rq}}{dt} + \omega_r \times \Phi_{rd} \end{cases} \tag{5.18}$$

- Stator Field:

$$\begin{cases} \Phi_{sd} = L_s \times I_{sd} + M \times I_{rd} \\ \Phi_{sq} = L_s \times I_{sq} + M \times I_{rq} \end{cases} \tag{5.19}$$

- Rotor Field:

$$\begin{cases} \Phi_{rd} = L_r \times I_{rd} + M \times I_{sd} \\ \Phi_{rq} = L_r \times I_{rq} + M \times I_{sq} \end{cases} \tag{5.20}$$

- Electromagnetic Torque:

$$C_{em} = p \times (\Phi_{sd} \times I_{sq} - \Phi_{sq} \times I_{sd}) \tag{5.21}$$

- The active and reactive powers of the stator:

$$\begin{cases} P_s = V_{sd} \times I_{sd} + V_{sq} \times I_{sq} \\ Q_s = V_{sq} \times I_{sd} - V_{sd} \times I_{sq} \end{cases} \tag{5.22}$$

- The active and reactive powers of the rotor:

$$\begin{cases} P_r = V_{rd} \times I_{rd} + V_{rq} \times I_{rq} \\ Q_r = V_{rq} \times I_{rd} - V_{rd} \times I_{rq} \end{cases} \tag{5.23}$$

5.4 Modeling of Power Converters

The converter powered by a source of perfect voltage imposes an AC voltage at its output, which is formed by a succession of two levels rectangular square waves, this

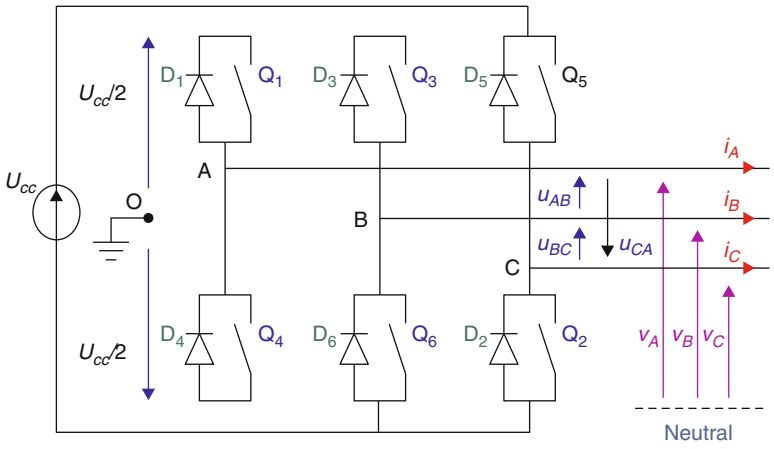

Fig. 5.11 Diagram of a three-phase voltage converter

being due to the opening and closing of the switches. The operating frequency is set by the control of the switches.

The three-phase system obtained at the output of the converter is a balanced voltage system containing odd harmonics that are different from rank three and their multiples (Mourad 2016).

The structural diagram of a three-phase voltage converter is given by Fig. 5.11.

The compound voltages are given by the following relations:

$$\begin{cases} U_{AB} = v_{AO} - v_{BO} \\ U_{BC} = v_{BO} - v_{CO} \\ U_{CA} = v_{CO} - v_{AO} \end{cases} \tag{5.24}$$

At the level of the charge, the simple voltages are giving as follows:

$$\begin{cases} U_{AB} = v_A - v_B \\ U_{BC} = v_B - v_C \\ U_{CA} = v_C - v_A \end{cases} \tag{5.25}$$

We have:

$$\begin{cases} U_{AB} - U_{CA} = 2v_A - (v_B + v_C) \\ U_{BC} - U_{AB} = 2v_B - (v_C + v_A) \\ U_{CA} - U_{BC} = 2v_C - (v_A + v_B) \end{cases} \tag{5.26}$$

The voltages (v_A, v_B, v_C) form a balanced three-phase system, so we can write:

$$\begin{cases} U_{AB} - U_{CA} = 3v_A \\ U_{BC} - U_{AB} = 3v_B \\ U_{CA} - U_{BC} = 3v_C \end{cases} \tag{5.27}$$

The expression of the simple voltages is presented by the following system (5.28)

$$\begin{cases} v_A = \frac{1}{3}(U_{AB} - U_{CA}) \\ v_B = \frac{1}{3}(U_{BC} - U_{AB}) \\ v_C = \frac{1}{3}(U_{CA} - U_{BC}) \end{cases} \tag{5.28}$$

Hence, the matrix form of simple voltages is giving as follows:

$$\begin{bmatrix} v_A \\ v_B \\ v_C \end{bmatrix} = \frac{1}{3}\begin{bmatrix} 2 & -1 & -1 \\ -1 & 2 & -1 \\ -1 & -1 & 2 \end{bmatrix}\begin{bmatrix} v_{AO} \\ v_{BO} \\ v_{CO} \end{bmatrix} \tag{5.29}$$

Each arm of the converter consists of two switches which are supposed perfect and operate in a complementary manner, it is therefore possible to associate a binary control (S_i) value with each arm with (i = A; B; C) and such that:

$$\begin{bmatrix} v_{AO} \\ v_{BO} \\ v_{CO} \end{bmatrix} = \frac{U_{CC}}{3}\begin{bmatrix} S_A \\ S_B \\ S_C \end{bmatrix} \tag{5.30}$$

By replacing the voltages with their values, we obtain:

$$\begin{bmatrix} v_A \\ v_B \\ v_C \end{bmatrix} = \frac{1}{3}\begin{bmatrix} 2 & -1 & -1 \\ -1 & 2 & -1 \\ -1 & -1 & 2 \end{bmatrix}\frac{U_{CC}}{3}\begin{bmatrix} S_A \\ S_B \\ S_C \end{bmatrix} \tag{5.31}$$

The simple voltages delivered by the converter will be obtained directly from the states of the control quantities S_A, S_B and S_C which represent the control signals of the switches.

The states of these quantities will also be determined by the envisaged control strategy.

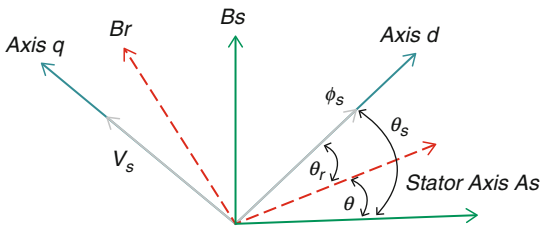

Fig. 5.12 Stator Field-orientation along the d axis

5.5 Field Oriented Control Strategy Applied to DFIG

5.5.1 Principle of Control by Field Orientation Control Strategy

The principle of control by field oriented control consists in orienting field along one of the axes in order to make the behavior of the induction machine similar to that of machine DC separately excited (Aimani 2004; Ihedrane et al. 2017a).

We have chosen to orient the stator field along the axis 'd' as shown in Fig. 5.12

According to this orientation we obtain:

$$\begin{cases} \Phi_{sd} = \Phi_s \\ \Phi_{sq} = 0 \end{cases} \tag{5.32}$$

In the referential (ABC), the voltage at the terminals of a phase 'i' of the stator is expressed as follows:

$$v_{si} = R_s \times I_{si} + \frac{d\Phi_{si}}{dt} \tag{5.33}$$

with: $i = 1, 2, 3$

Assuming the resistance of the stator winding 'R_s' is negligible for the medium and high power machines generally employed in the wind energy conversion (Ihedrane et al. 2017a; Mourad 2016), we obtain:

$$v_{si} = \frac{d\Phi_{si}}{dt} \tag{5.34}$$

We supposed that the voltages of the electrical grid are stable; the stator flux will also be constant. So, we can write:

$$\begin{cases} v_{sd} = 0 \\ v_{sq} = v_s = \omega_s \times \Phi_s \end{cases} \tag{5.35}$$

We have chosen to orient the stator flux along the axis 'd', we obtain:

$$\begin{cases} I_{sd} = \dfrac{1}{L_s} \times (\Phi_s - M \times I_{rd}) \\ \\ I_{sq} = -\dfrac{M}{L_s} \times I_{rq} \end{cases} \tag{5.36}$$

So, the previous relations become as follows:

- Relation between the electromagnetic torque and the rotor currents:
  The expression of the torque is written as follows:

$$C_{em} = p \times I_{sq}.\Phi_s = -p \times \frac{M}{L_s} \times \Phi_s \times I_{rq} \tag{5.37}$$

- Relation between stator powers and rotor currents:
  We replaced I_{sq} and I_{sd} by their expressions in the expression of the stator power (P_s and Q_s) and knowing that $v_{sd} = 0$,the expression of the active and reactive stator powers become as follows:

$$\begin{cases} P_s = V_{sq} \times I_{sq} = -V_s \times \dfrac{M}{L_s} \times I_{rq} \\ \\ Q_s = V_s \times I_{sd} = \dfrac{V_s^2}{\omega_s \times L_s} - V_s \times \dfrac{M}{L_s} \times I_{rd} \end{cases} \tag{5.38}$$

- Relation between rotor voltage and rotor current:
  By replacing I_{sq} and I_{sd} with their expressions in Φ_{rd} and Φ_{rq} we get:

$$\begin{cases} \Phi_{rd} = (L_r - \dfrac{M^2}{L_s}) \times I_{rd} + \dfrac{M \times v_s}{L_s \times \omega_s} \\ \\ \Phi_{rq} = (L_r - \dfrac{M^2}{L_s}) \times I_{rq} \end{cases} \tag{5.39}$$

By injecting these equations into the expressions of the rotor voltages, we obtain the following expression:

$$\begin{cases} V_{rd} = \left[R_r + S \left(L_r - \dfrac{M^2}{L_s} \right) \right] I_{rd} - \omega_s \, g \, \left(L_r - \dfrac{M^2}{L_s} \right) \, I_{rq} \\ \\ V_{rq} = \left[R_r + S \left(L_r - \dfrac{M^2}{L_s} \right) \right] I_{rq} - \omega_s \, g \, \left(L_r - \dfrac{M^2}{L_s} \right) I_{rd} + \dfrac{g \, M \, V_s}{L_s} \end{cases} \tag{5.40}$$

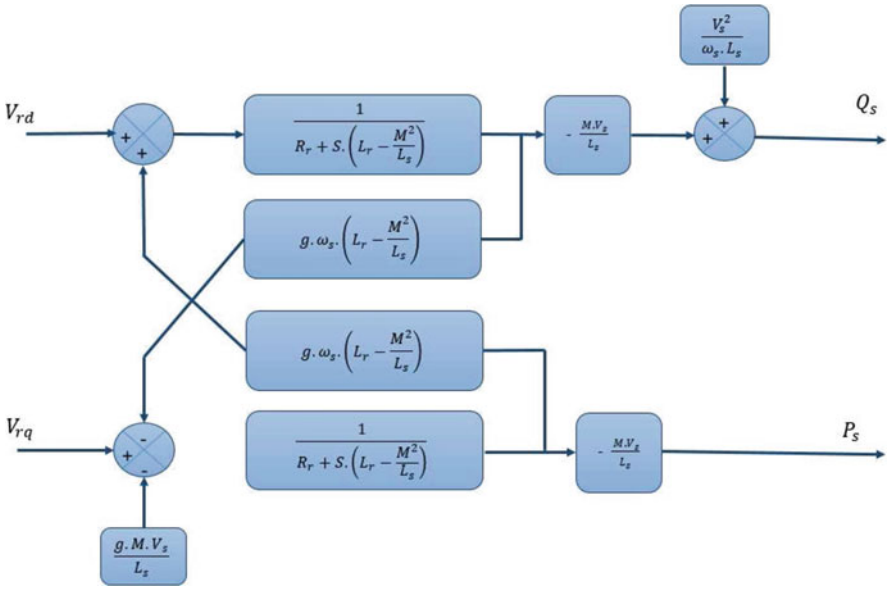

Fig. 5.13 Simplified model of the DFIG

with:

g: the slip of the induction machine.

$\omega_r = g \times \omega_s$: the rotor pulsation

ω_s: The stator pulsation

These equations make it possible to establish a block diagram of the electrical system that can be regulated (Fig. 5.13):

According to this block diagram, we can note that the rotor voltages and the stator powers are linked by transfer functions with the first order. This allows to set up a vector control with the influence of the couplings, each axis can be controlled independently with its own controller.

For these controllers, the reference values will be the active power for the rotor axis 'q' and the reactive power for the rotor axis 'd' (Allam et al. 2014; Poitiers 2003).

The reactive power reference will be kept zero in order to ensure a unit power factor on the stator side so as to optimize the quality of the energy sent to the grid. The active power reference should allow keeping the wind power factor optimal.

To carry out the power control of this machine, there are two structures:

- Structure of the direct control.
- Structure of the indirect control.

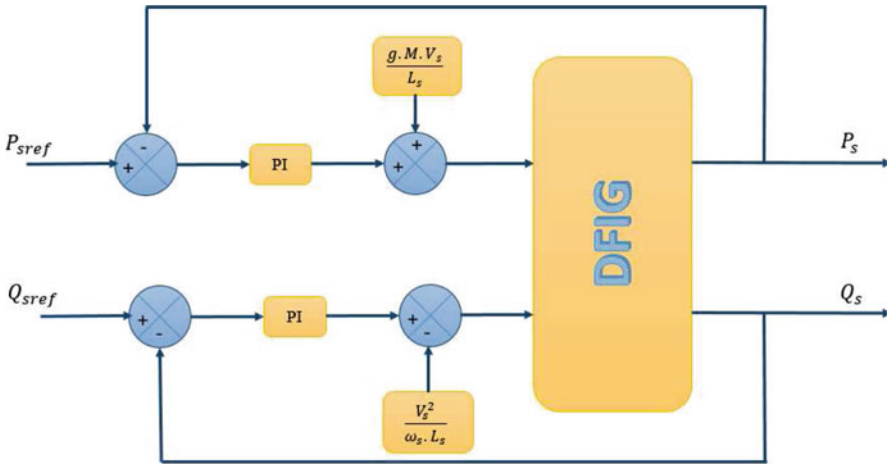

Fig. 5.14 Direct control of the doubly fed induction generator

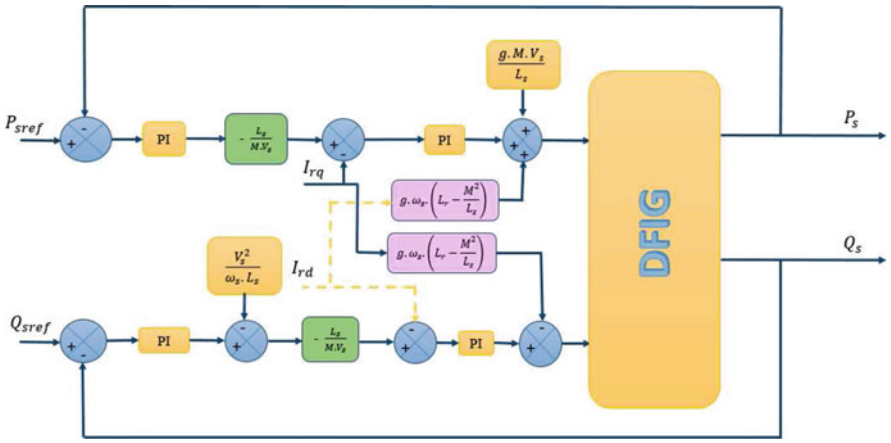

Fig. 5.15 Indirect control of the doubly fed induction generator

5.5.1.1 Structure of Direct Control

The block diagram of the direct control of the Doubly Fed Induction Generator is shown in Fig. 5.14.

This method consists in neglecting the coupling terms and setting up a regulator on each axis in order to control independently the active and reactive powers (Sejir 2006; Tarfaya et al. 2015).

5.5.1.2 Structure of Indirect Control

The indirect control of the Doubly Fed Induction Generator is given by Fig. 5.15.

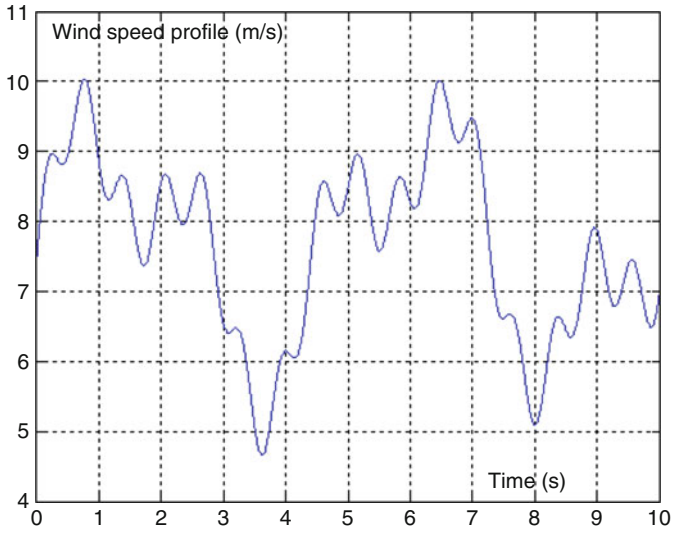

Fig. 5.16 Wind profile

The second method consists in considering the coupling terms and compensates them by performing a system with two loops in order to control the powers and the rotor currents. This technique wich called indirect method, allows to controlling the rotor currents in order to ensure protection of the generator DFIG by limiting the currents and giving more flexibility to the machine (Allam et al. 2014; Ihedrane et al. 2017a).

5.6 Simulation and Interpretations

In order to examine the robustness of the Field Oriented Control Technique with the turbine control by the MPPT strategy, we applied a random wind profile given by Fig. 5.16.

The rotational speed of the DFIG (Fig. 5.17) has less oscillation and high reliability with respect to wind speed profile (Fig. 5.16).

5.6.1 Simulation Result of the Direct Field Oriented Control DFOC

Figure 5.18 shows the simulation results of Direct Field Oriented Control DFOC:

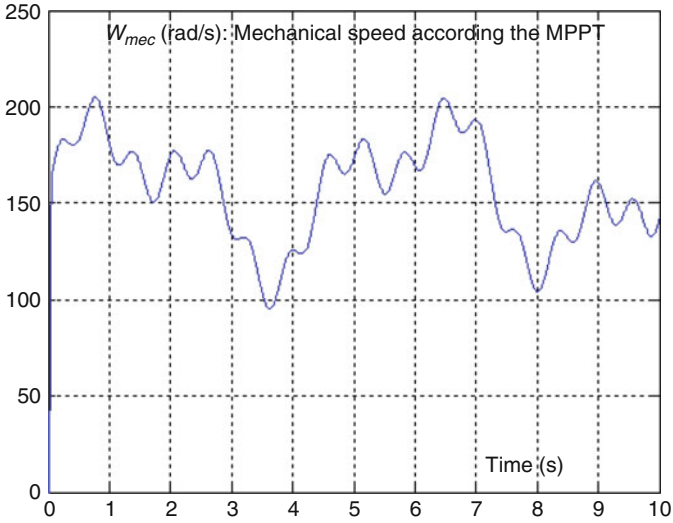

Fig. 5.17 Rotational speed of the DFIG ω_{mec}

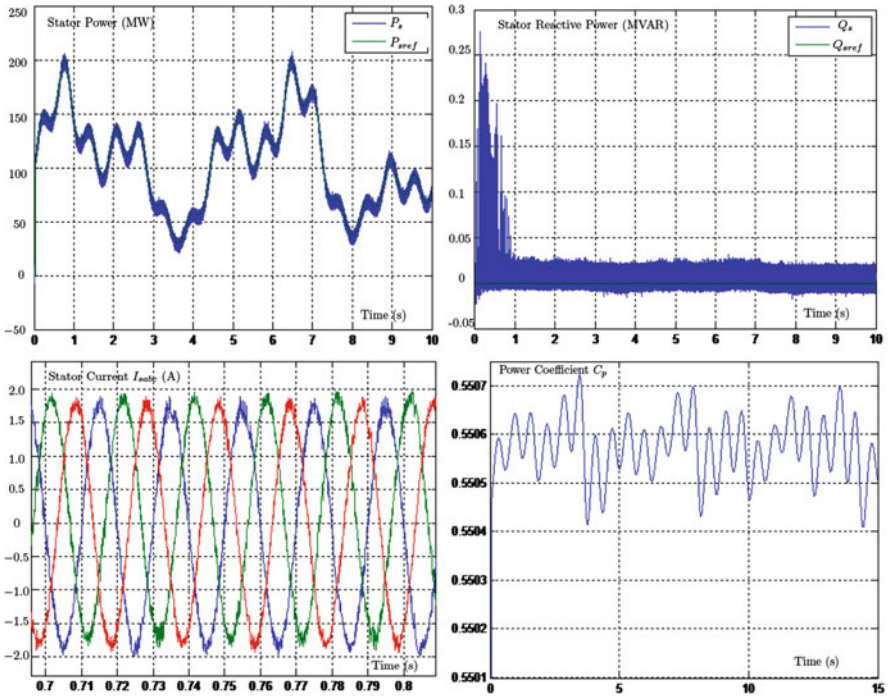

Fig. 5.18 Simulation results of direct field oriented control

- The active power (a) follows its reference values (which is the mechanical power obtained according to the MPPT control strategy) for all the variations of the wind, which shows the robustness of the field oriented control of the DFIG during the variation of the wind speed.
- The stator reactive power (b) is maintained at zero in order to ensure a unit power factor on the stator side.
- The output currents I_{sabc} (c) in the wind system is almost sinusoidal with a fixed frequency equivalent to that of the grid ($50H_z$), which implies a good injection into the grid.
- The power coefficient C_p(d) reach its maximum values $C_p = 0.5505$, which implies that the system provide an optimal power from the wind.

5.6.2 *Simulation Result of the Indirect Field Oriented Control IFOC*

Figure 5.19 presents the different performances of the Indirect Field Oriented Control, which shows the robustness of the wind system and the good tracking.

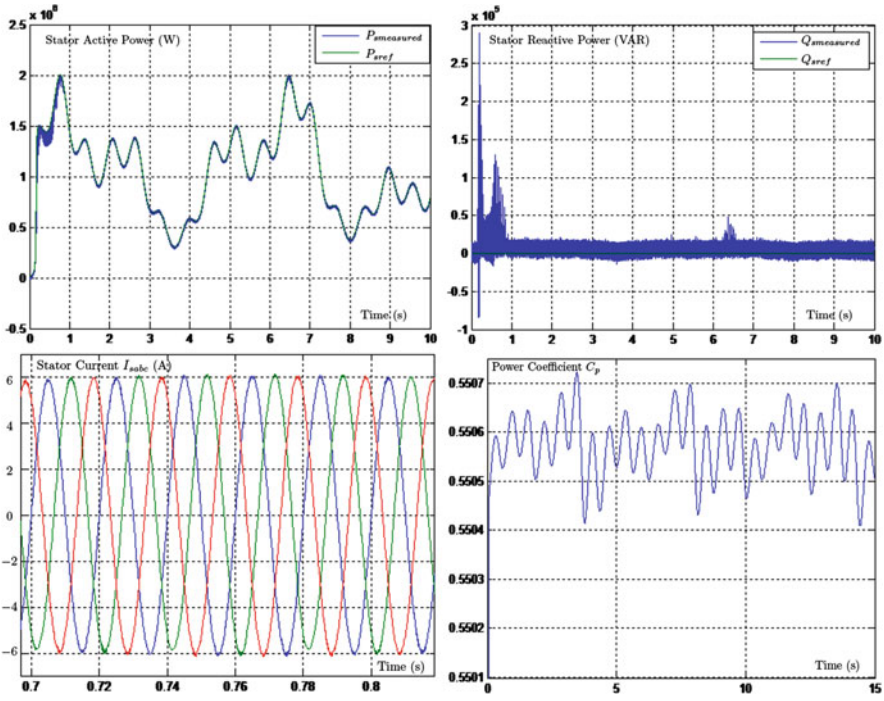

Fig. 5.19 Simulation results of indirect field oriented control IFOC

- The stator active and reactive power (a, b) show a perfect decoupling and a good tracking of their references values with a reduction of the undulations, compared to the direct control. Consequently, the harmonics are minimized.
- The stator currents (c) are also sinusoidal in shape, with an improvement in quality compared to those obtained by the direct control, which implies a clean power without harmonics echanged between the DFIG and the grid.
- From (d) we can note that the power coefficient kept around its optimum $C_{pmax} = 0.5505$.

So, the results obtained from the IFOC show the reliability and robustness of the proposed control and provide better control for injecting power into the grid.

5.7 Conclusion

This work has been devoted to the modeling and control of the wind turbine conversion system based on the doubly-fed induction generator DFIG in order to regulate the active and reactive stator power, with the MPPT strategy to extract the maximum of the power generated by DFIG.

Thus, we presented two methods of control of the DFIG which were implemented under MATLAB/SIMULINK in order to visualize the results of simulation.

Direct methods in which the active and reactive powers are measured and compared with their references. The indirect method has the role to improve the tracking of the instructions and therefore, ameliorate the performance of the wind system.

We have seen that the direct control has good results with low implementation complexity, On the other hand, the indirect method allows to obtain an efficient and robust system. It is true that it is more complex but it makes possible to achieve an optimal operation of the electrical generation system by minimizing the worries linked to the parametric variations of the DFIG.

As perspective, this work can be continued and completed by the implementation of this command in an FPGA.

References

Aimani, S. E. (2004). *Modélisation de Différentes Technologies d'Eoliennes Intégrées dans un Réseau de Moyenne Tension*. Ph.D. thesis, Université des Sciences et Technologies de Lille.

Allam, M., Dehiba, B., Abid, M., Djeriri, Y., & Adjoudj, R. (2014). Etude comparative entre la commande vectorielle directe et indirecte de la machine asynchrone à double alimentation(mada) dédiée à une application éolienne. *Journal of Advanced Research in Science and Technology, 1*(2), 88–100.

Bossoufi, B., Karim, M., Lagrioui, A., Taoussi, M., & Hafyani, M. (2014). Backstepping control of DFIG generators for wide-range variable-speed wind turbines. *IJAAC International Journal of Automation and Control, 8*(2), 122–140.

Bekakra, Y., & Attous, D. B. (2011). Sliding mode controls of active and reactive power of a DFIG with MPPT for variable speed wind energy conversion. *Australian Journal of Basic and Applied Sciences, 5*, 2274–2286.

Bennani, H. (2011). *Machine asynchrone à double alimentation: Les lois de commande en régime permanent*. Ph.D. thesis, Université de Laval, Québec.

Datta, R., & Ranganathan, V. R. (2002). Variable-speed wind power generation using doubly fed wound rotor induction machine a comparison with alternative schemes. *IEEE Transaction on Energy Conversion, 17*, 414–421.

de Wit, C. C. (2000). Commande des moteurs asynchrone modélisation contrôle vectoriel et DTC. *Lavoisier, 1*, 10–22.

Gaillard, A. (2010). *Systéme éolien basé sur une MADA: Contribution l'étude de la qualité de l'énergie électrique et de la continuité de service*. Ph.D. thesis, Université Henri Poincaré, Nancy-I.

Ghoudelbourk, S., Dib, D., Omeiri, A., & Azar, A. T. (2016). MPPT control in wind energy conversion systems and the application of fractional control (PI^{α}) in pitch windturbine. *International Journal of Modelling, Identification and Control, 26*, 140–151.

Guda, S. R. (2005). *Modeling and power management of a hybrid wind-microturbine power generation*. Master's thesis, Université de Bozeman, Monata.

Ihedrane, Y., Chakib, E., & Bossoufi, B. (2017a). Power control of DFIG-generators for wind turbines variable-speed. *International Journal of Power Electronics and Drive Systems (IJPEDS), 8*(1), 444–453.

Ihedrane, Y., Chakib, E., & Bossoufi, B. (2017b). Direct and indirect field oriented control of DFIG-generators for wind turbines variable-speed. In *IEEE 14th International Multi-Conference on Systems, Signals & Devices*, Marrakech, Morocco (pp. 27–32).

Johansen, P. R., Patterson, D., O'Keefe, C., & Swenson, J. (2001, January–March). The use of an axial flux permanent magnet in wheel direct drive in an electric bicycle. *Renewable Energy, 22*(1–3), 151–157.

Kazemi, M. V., Yazdankhah, A. S., & Kojabadi, H. M. (2010). Direct power control of DFIG based on discrete space vector modulation. *Renewable Energy, 35*, 1033–1042.

Mourad, L. (2016). *Synthèse de lois de commande non-linéaires pour le contrôle d'une machine asynchrone à double alimentation dédiée à un système aérogénérateur*. Ph.D. thesis, Université Aboubakr Belkaid – Tlemcen – Faculté de Technologie.

Park, R. H. (2012). Two-reaction theory of synchronous machines: Generalized method of analysis – Part I. In *Transaction of the AIEE, 48*, 716–730.

Poitiers, F. (2003). *Etude et commande de génératrice asynchrones pour l'utilisation de l'énergie éolienne*. Ph.D. thesis, Ecole polytechnique de l'Université de Nantes.

Sejir, K. (2006). *Commande Vectorielle d'une Machine Asynchrone Doublement Alimentée (MADA)*. Ph.D. thesis, Institut National Polytechnique de Toulouse, France.

Tarfaya, A., Dib, D., & Ouada M. (2015). Variable-speed wind power generation using doubly fed wound rotor induction machine a comparison with alternative schemes. *International Conference on Mechanical And Industrial Engineering ICMAIE'2015*, Kuala Lumpur, Malaysia.

Youcef, B. (2014). *Contribution à l'étude et à la Commande Robuste d'un Aérogénérateur Asynchrone à Double Alimentation*. Ph.D. thesis, Université Mohamed Khider – Biskra.